ACS Catalysis

Research Article

pubs.acs.org/acscatalysis

Use of Short Time-on-Stream Attenuated Total Internal Reflection Infrared Spectroscopy To Probe Changes in Adsorption Geometry for Determination of Selectivity in the Hydrogenation of Citral

H. Daly,[†] H. G. Manyar,[†] R. Morgan,[†] J. M. Thompson,[†] J.-J. Delgado,[‡] R. Burch,[†] and C. Hardacre*[,†]

[†]CenTACat, School of Chemistry and Chemical Engineering, Queen's University Belfast, BT9 5AG, United Kingdom

[‡]Departamento de Ciencia de los Materiales e Ingeniería Mmetallurgica y Química Inorgánica, Universidad de Cádiz, Puerto Real, Cádiz, Spain

Supporting Information

ABSTRACT: A new experimental procedure based on attenuated total reflection infrared spectroscopy has been developed to investigate surface species under liquid phase reaction conditions. The technique has been tested by investigating the enhanced selectivity in the hydrogenation of α,β-unsaturated aldehyde citral over a 5% Pt/SiO_2 catalyst toward unsaturated alcohols geraniol/nerol, which occurs when citronellal is added to the reaction. The change in selectivity is proposed to be the result of a change in the citral adsorption mode in the presence of citronellal. Short time on stream attenuated total internal reflection infrared spectroscopy has allowed identification of the adsorption modes of citral. With no citronellal, citral adsorbs through both the C═C and C═O groups; however, in the presence of citronellal, citral adsorption occurs through the C═O group only, which is proposed to be the cause of the altered reaction selectivity.

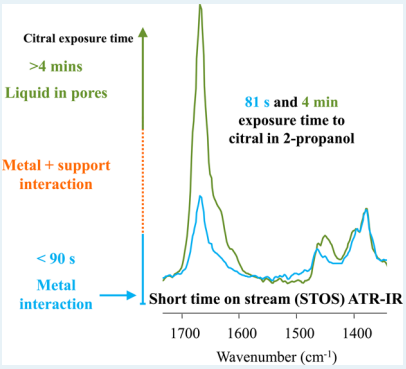

KEYWORDS: *Pt, ATR, infrared, citral, hydrogenation*

INTRODUCTION

In chemoselective hydrogenations, such as the hydrogenation of α,β-unsaturated aldehydes, there is the desire to understand and control the reaction pathway so as to obtain a specific product with high selectivity. The hydrogenation of citral is of particular interest because of the complex reaction network resulting from the preferential adsorption geometry and strength of interaction of different functional groups within the molecule, namely the C═O, conjugated C═C, and isolated C═C bonds the hydrogenation and further reaction of which can form a wide range of products illustrated in Scheme 1. The hydrogenation of citral has been studied extensively with the choice of metal, support, reaction conditions, and solvent all reported to affect the selectivity.[1] With unsaturated alcohols being important fine chemical and pharmaceutical intermediates, there is significant interest in improving the selectivity to these desired products. Modification of the catalyst through addition of a second metal, such as Sn, Fe or Ge, has been reported to alter reaction selectivity toward C═O hydrogenation.[2] For other chemoselective hydrogenations, modification of the catalyst surface via the adsorption of organic compounds has also been reported, with *n*-alkanethiol self-assembled-monolayer-coated Pd catalysts and thiol-modified Pt/TiO_2 catalysts giving excellent selectivity enhancements in hydrogenation of unsaturated epoxides to saturated epoxides[3] and a complete switch in the products formed for 4-nitrostyrene hydrogenation following modification, respectively.[4]

The attainment of higher selectivity upon addition of an organic compound into the liquid phase reaction has also been reported for the hydrogenation of citral. The addition of thiophene to Ru/KL catalysts gave a maximum selectivity to geraniol and nerol of 46% (at 15% citral conversion with 3 ppm thiophene); in the absence of the thiophene, the Ru catalysts typically favor C═C hydrogenation.[5] Therein, it was also reported that the adsorption mode of the thiophene (relating to thiophene concentration/surface coverage) altered whether the citral adsorbed through the C═C or the C═O bond. Addition of ethylenediamine during the hydrogenation of citral over a Ru/AlO(OH) catalyst (in water) resulting in 87% selectivity to geraniol/nerol (93% conversion), whereas selectivity of 74.3% (at 60.5% conversion) was obtained without the additive.[6] Similar effects have been observed with Pt-based catalysts with both amines[7] and thiols,[8] resulting in enhancements to the unsaturated alcohol selectivity.

In this study, we report the hydrogenation of citral with a selectivity of 97% to geraniol and nerol at 100% conversion over a Pt/SiO_2 catalyst when citronellal (a minor reaction product) is added to the reaction; the adsorption of citronellal influences the adsorption of citral, favoring C═O hydrogenation. It is evident that the adsorption geometry of the reagent is critical in

Received: February 12, 2014
Revised: June 13, 2014
Published: June 16, 2014

   dx.doi.org/10.1021/cs500185n | ACS Catal. 2014, 4, 2470−2478

Scheme 1. Reaction Scheme for the Hydrogenation of Citral

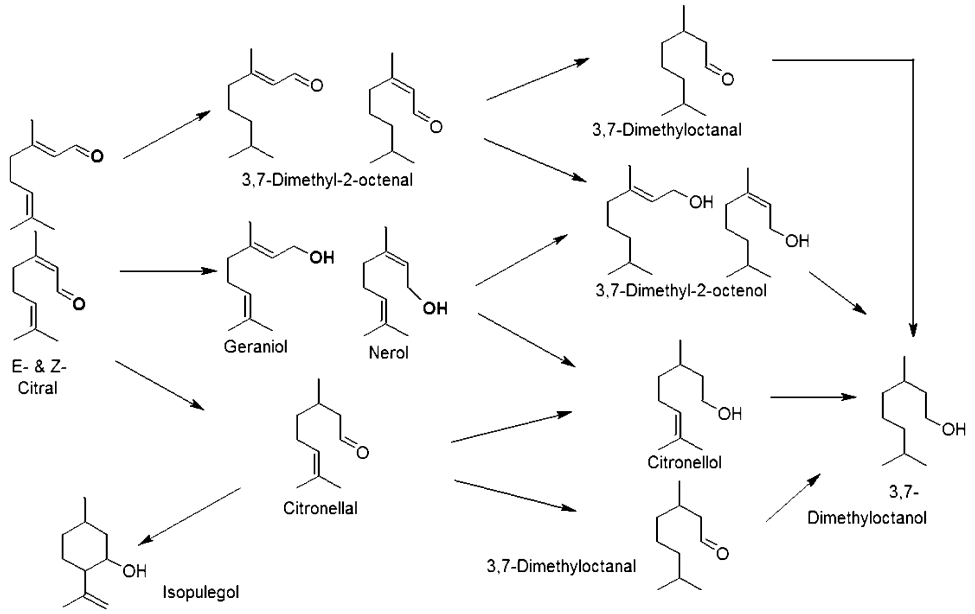

determining the reaction selectivity, and in this study, attenuated total internal reflection infrared (ATR-IR) spectroscopy is used to probe the mode of citral adsorption and modification of this adsorption mode in the presence of citronellal.

Differentiating between potential reaction intermediates and inactive spectrator species for catalytic reactions in the liquid phase is very challenging. A technique of choice in the study of the catalyst−liquid interface over the past decade has been ATR-IR spectroscopy.[9] The use of model metal films[10] or catalyst/reagent systems in which no support adsorption occurs[11] has been reported and enabled spectra showing interaction with only the metal to be directly obtained. However, for powdered catalyst films, there are limitations of the technique in terms of identifying the relevant species associated with the active metal in spectra that also contain contributions from species dissolved in the liquid phase (within the catalyst pores and in the interparticle void volume[12]) as well as species adsorbed on the support. Liquid phase contributions and support adsorption can dominate spectra for supported metal catalysts because most of the surface area probed by the IR beam will be associated with the support compared with the contribution from adsorption on the metal.[13]

Modulation excitation spectroscopy with phase-sensitive detection coupled with ATR-IR spectroscopy has been developed to probe species adsorbed on the catalyst, being applied to both model metal and catalyst films, for systems such as alcohol oxidation[14] and adsorption of chiral modifiers on Pt or Pd for chemoselective hydrogenations.[15] Other methods (both experimental and analytical) to overcome the limitation and distinguish adsorption on the metal in the presence of contributions from the liquid/support adsorption include performing reactions with two ATR-IR probes. Therein, one was coated with catalyst and the other used to monitor the dissolved species during the reaction.[16] Sun and Williams recorded "blank" experiments for reagents in the liquid over the support and the catalyst and then deconvoluted the spectra to distinguish adsorption on the metal.[17]

Time-resolved ATR-IR spectra have been reported in the study of pure ethanol (and ethanol/2-propanol) oxidation over Pd/Al_2O_3.[18] On switching from H_2- to O_2-saturated ethanol, transient species such as ethyl acetate are identified in the liquid phase together with the primary oxidation product acetaldehyde, which continues to form under an O_2 environment. Adsorption of acetate on the support and CO on the Pd are also observed, which shows that oxidation (to acetic acid) and decarbonylation of the acetaldehyde also occur. Ethyl acetate formation via acetic acid is also proposed from the response of dissolved ethyl acetate and acetate on the support directly following the switch to O_2-saturated ethanol, showing the need for rapid monitoring of reactions. This technique has also been applied to the aqueous phase reforming of glycerol over Pt/Al_2O_3.[19] By switching between feeds containing water, water + glycerol, water + O_2, and water + H_2, the rate of formation of CO from the reaction of glycerol on various pretreated surfaces can be examined. In addition, from a comparison of the linear and bridge-bound CO formed, on switching from the glycerol feed to pure water, the bridge-bound species was found to react via the water gas shift reaction, whereas little change with time was observed for the linear species.

Recently, the application of a short time-on-stream (STOS) technique coupled with diffuse reflectance infrared fourier transform (DRIFT) spectroscopy has been shown to be effective in the gas phase for hydrocarbon selective catalytic reduction of NO over Ag catalysts.[20] Therein, it was possible, by limiting the exposure time of the catalyst to the reaction feed, to differentiate the species adsorbed on the metal and the support. In this case, the observation in the spectroscopy of accumulated spillover spectator species from the metal onto the support was decreased by examining the surface species only during the first few seconds following initiation of the reaction. In this paper, we have applied the short time on stream (STOS-ATR-IR) methodology to examine the liquid phase adsorption of an α,β-unsaturated aldehyde on a Pt/SiO_2 catalyst. Herein, by limiting the exposure of the catalyst to the reagent in solution, it is possible to detect species adsorbed on the metal before support

dx.doi.org/10.1021/cs500185n | ACS Catal. 2014, 4, 2470−2478

adsorption, and contributions from the liquid phase species dominate the spectra.

Although the hydrogenation of citral has been widely studied, there are limited studies probing the adsorption geometry of citral, in comparison with other α,β-unsaturated aldehydes. Density functional theory (DFT) studies on the effect of amine capping agents on reaction selectivity for amine-capped PtCo nanocrystals[7] and the effect of solvent on the hydrogenation of the isolated versus conjugated C=C bonds in citral[21] have been reported. In addition, infrared spectroscopy for the adsorption of citral on Rh and Pt blacks[22] and ATR-IR spectroscopy to study the deactivation over a Pd/Al_2O_3 catalyst[23] have been studied. In the ATR-IR study, adsorption of CO on Pd from decarbonylation of citral was observed during the reaction. Additional species in the ATR-IR spectra due to citral dissolved in the solvent and adsorbed on the alumina support, as well as dissolved products (citronellal/dihydrocitronellal), carboxylate species, and bands between 1300 and 1450 cm^{-1} due to unassigned adsorbed species were observed. The interaction of citral with Pd was not observed therein.

Because the adsorption geometry is clearly critical in determining the ultimate selectivity, it is important to be able to probe this adsorption on the metal, in particular, using a real catalyst in the presence of the solvent. Therefore, we have applied STOS-ATR-IR coupled with site-blocking with CO[24] to distinguish signals from citral adsorption of Pt from adsorption on the silica support as well as citral in the liquid phase. This has provided information that has been used to understand the reaction selectivity in the hydrogenation of citral to geraniol and nerol and changes in adsorption geometry that occur under different surface modifications.

EXPERIMENTAL SECTION

Citral hydrogenation reactions were carried out in the kinetic regime, free from mass transfer limitations using a 100 cm^3 Autoclave Engineer's high-pressure reactor charged with 0.02 mol of citral (96%, Alfa Aesar) and 0.3 g of 5% Pt/SiO_2 catalyst (Johnson Matthey) suspended in 60 cm^3 of 10 mol % 2-propanol in water. The reactor was purged three times with N_2 before heating to 100 °C with the reaction mixture agitated at 1500 rpm. After purging with H_2 (high purity from BOC) three times, the reactor was pressurized to 1 MPa, which corresponds to $t = 0$. The reaction was monitored by sampling at regular intervals with GC analysis of the samples (DB-1 capillary column and FID detector). The catalyst recycle was performed by removal of the catalyst from the reaction mixture by filtration. The catalyst was then washed with IPA and dried at 120 °C before being reused. In the spiking experiments, 0.003 mol of citronellal was added to the citral/solvent reaction mixture and the reaction was performed as before.

Hydrogenation reactions were also performed in pure 2-propanol, and the same conversion-selectivity profiles were observed with and without spiking with citronellal. Because of the strong adsorption bands from water, all the ATR-IR spectroscopic measurements were performed using 2-propanol rather than 2-propanol/water mixtures.

DRIFT spectra of citral adsorbed on SiO_2 (Davicat) and Pt/SiO_2 were collected using a Collector II accessory with an environmental chamber (Spectra-Tech) in a Vertex 70 infrared spectrometer (Bruker). Prior to exposure to citral, the Pt/SiO_2 catalyst was reduced at 100 °C in 10% H_2 in Ar (50 cm^3 min^{-1}) for 1 h, and the gas was switched to Ar and cooled to 30 °C for the adsorption study. The SiO_2 catalyst was heated under Ar to 100 °C and held for 1 h. The reduced Pt/SiO_2 and dried SiO_2 at 30 °C were used for their respective background spectra. Citral was delivered to the cell by means of a saturator system with an Ar flow (20 cm^3 min^{-1}, saturator temperature of 25 °C), which corresponded to 200 ppm of citral. Spectra were recorded with 1024 scans at 4 cm^{-1} resolution every 5 min over a 30 min period.

ATR-IR spectra were recorded using a PIKE ATRMax II accessory in a Vertex 70 infrared spectrometer (Bruker) over a ZnSe internal reflection element (IRE) or ZnSe coated with Pt/SiO_2 catalyst. The Pt/SiO_2 catalyst layers were prepared by grinding the catalyst and forming a suspension in ultrapure water (0.25 g of catalyst/10 g of water). The solution was then sonicated for 10 min immediately before slurrying 1 cm^3 onto the ZnSe IRE. Thereafter, the film was left in air to dry for 15 h. This catalyst film was used as background, and all spectra were recorded with 32 scans at 4 cm^{-1} resolution. Importantly, although the depth of penetration of the IR beam into a 2-propanol-saturated 5% Pt/SiO_2 layer is ~1.5 μm at 1000 cm^{-1}, the thickness of the deposited layers exceeds this value (~100 μm), and the particles are also crushed and sieved to <45 μm, so the catalyst particle size is, on average, much greater than the depth of penetration of the beam. The catalyst layers were found to be stable and reproducible with comparable intensities for bands due to 2-propanol obtained in each experiment for each new layer of catalyst that was deposited. No catalyst particles were detected in the outlet of the flow cell, and the layers were intact following each experiment.

Solutions (0.1 M) of citral and citronellal (96%, Alfa Aesar) in 2-propanol (>99.8% from Sigma-Aldrich, used as received) were passed over the catalyst using an in-house flow-through cell at 0.5 cm^3 min^{-1}, and the liquid flow was controlled by metering valves (Swagelok). To equilibrate the catalyst to the solvent, 2-propanol was flowed over the catalyst for 15 min (a steady signal for 2-propanol observed after this time), and then the feed was switched, using an 8 position electrically actuated fast switching valve from Vici, to 0.1 M citral or citronellal solutions with spectra collected every 27 s for the desired time. To distinguish the adsorption of the compounds on the Pt from the SiO_2 support, CO was preadsorbed onto the catalyst. CO was bubbled through 2-propanol for 30 min before being flowed over the catalyst for 90 min, at which point no further changes to the spectra were observed. The flow was then switched to a pure 2-propanol feed for 15 min to purge the cell of CO and remove any weakly bound CO. Thereafter, the feed was switched to expose the catalyst to 0.1 M citral or citronellal in 2-propanol.

To probe the effect of citronellal on the adsorption of citral, 0.1 M citronellal/2-propanol was flowed over the Pt/SiO_2 film for 25 min before switching the feed to 0.1 M citral/2-propanol and recording spectra every 27 s following the switch.

In the ATR-IR experiments, the catalyst was reduced by flowing the 2-propanol over the catalyst film prior to switching the feed to citral, citronellal, or CO. This reduction procedure was utilized in the ATR-IR experiments, as opposed to using hydrogen dissolved in the solvent, to avoid significant amounts of hydrogen adsorbed on the Pt being present. This hydrogen would react with the citral on switching to the citral feed and complicate the spectra as a result of the presence of bands due to both products and citral adsorption. It should also be noted that the citral hydrogenation reaction was also performed without prior reduction of the catalyst, and no effect on the rate

dx.doi.org/10.1021/cs500185n | ACS Catal. 2014, 4, 2470−2478

or selectivity was observed. A schematic of the ATR-IR reactor setup is shown in Figure 1.

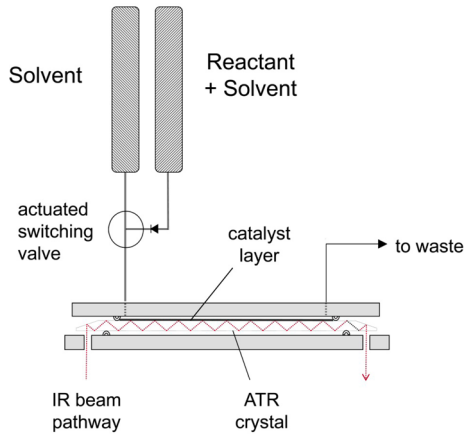

Figure 1. Schematic of ATR-IR reactor setup.

RESULTS AND DISCUSSION

The selective hydrogenation of citral using a 5% Pt/SiO_2 catalyst has been studied, and the time profile is shown in Figure 2a. A 97% selectivity to gernaiol/nerol at 100% conversion for the reaction performed in water/2-propanol (9:1 mol ratio) was observed (Figure 2). It should be noted that with the exception of the formation of citronellal and geraniol/nerol, all other products made up <1% of the composition in the liquid phase. The higher apparent citral conversion observed in the initial 60 min of reaction is thought to be due to adsorption of citral on the catalyst. For example, after 10 min of reaction, 1.74×10^{-3} mol of citral is found to be converted into products, indicating that 2.48×10^{-3} mol of citral is not observed because of adsorption; that is, the mass balance was ~86.9% at the early stages of reaction. This is consistent with adsorption isotherms measured using the same mass of catalyst that showed 2.6×10^{-3} mol of citral was adsorbed on the metal and support. In this adsorption-dominated period of the reaction, up to 60 min of the reaction, the selectivity gradually increased from 70% to geraniol/nerol and 30% to citronellal at 10 min and, as the reaction proceeded to 100% conversion, the selectivity to geraniol/nerol increased to 97%. Thereafter, the mass balance increased, and by 180 min of reaction, 97% of the molecules were accounted for. At this point, some of the citronellal formed at the start of the reaction was not observed in the liquid phase and is thought to be adsorbed on the catalyst. Interestingly, on recycling the catalyst, enhanced selectivity to geraniol/nerol was observed from the start of the reaction (Figure 3), indicating that the adsorbed species at the end of the first reaction modifies the surface of the catalyst.

To examine whether this could be due to citronellal adsorption, a fresh catalyst−solvent mixture was spiked with citronellal. After spiking the reaction mixture with citronellal, the minor reaction product, selectivities of >97% to gernaiol/nerol from the start of the reaction were observed (Figure 2b). Therefore, it is postulated that the citronellal product adsorbs onto the catalyst, altering the mode of citral adsorption and thus increasing the selectivity for C═O rather than C═C hydrogenation either through templating the surface or adsorbing on unselective sites. In the present paper, this effect

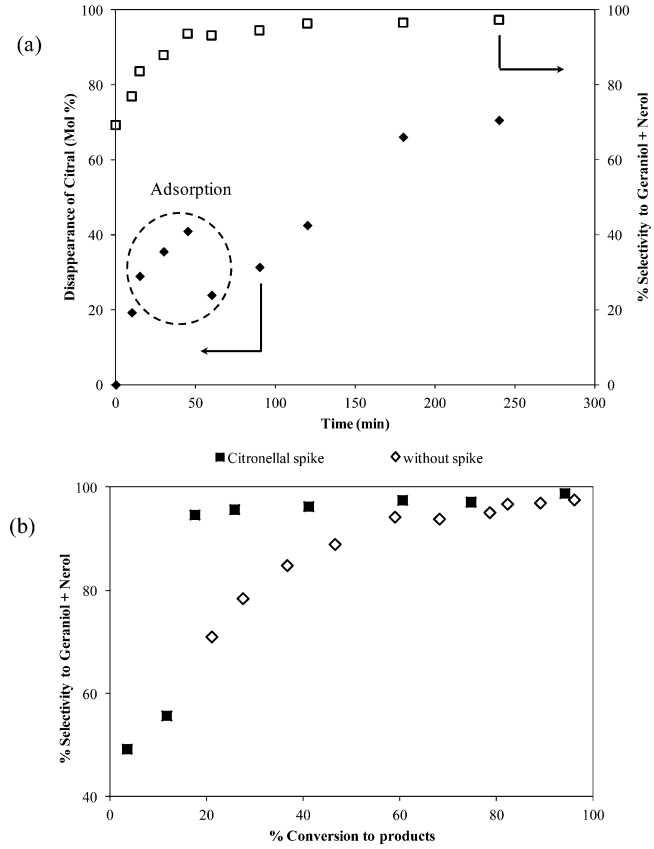

Figure 2. (a) Percent disappearance of citral from the liquid phase during the hydrogenation, in mol % (♦), and selectivity to geraniol + nerol (□) as a function of reaction time. (b) Comparison of percent selectivity of geraniol + nerol during citral hydrogenation with a fresh catalyst (◇) and after the reaction is spiked with 15 mol % citronellal (■) as a function of percent conversion to products calculated from product concentrations in the liquid phase. Reaction conditions: citral, 0.02 mol; solvent, 60 cm^3 (10 mol % 2-propanol in water); 5% Pt/SiO_2 catalyst, 0.3 g (particle size <45 μm); 100 °C; H_2 pressure, 1 MPa; stirrer speed, 1500 rpm.

has been probed using DRIFT and ATR-IR spectroscopy coupled with the liquid phase STOS technique.

Figure 4 shows that when using conventional DRIFT spectroscopy, no significant differences after adsorption of gas phase citral on the Pt/SiO_2 catalyst compared with the blank SiO_2 are observed. In addition, after blocking the Pt by adsorption of CO, similar spectra are obtained for the catalyst and the blank support. This indicates that the conventional DRIFT spectra are dominated by the interaction between the citral and silica and, therefore, cannot be used to probe the surface interaction with the active site.

To investigate the adsorption in the presence of the 2-propanol solvent, ATR-IR spectroscopy was used. In these experiments, the solvent was equilibrated with the catalyst layer on the ATR crystal using a flow cell, after which the feed was switched to a solution of 0.1 M citral in 2-propanol. The subsequent ATR-IR spectra of citral on the Pt/SiO_2 catalyst are shown in Figures 5 and S1 (Supporting Information; SI) for different exposure times to the feed.

At long exposure times (SI Figure S1), the bands observed on the catalyst film were comparable to those found in the liquid phase citral spectrum over the blank ZnSe crystal, both in position and relative intensity (Figure 5). In this case, it is

dx.doi.org/10.1021/cs500185n | ACS Catal. 2014, 4, 2470−2478

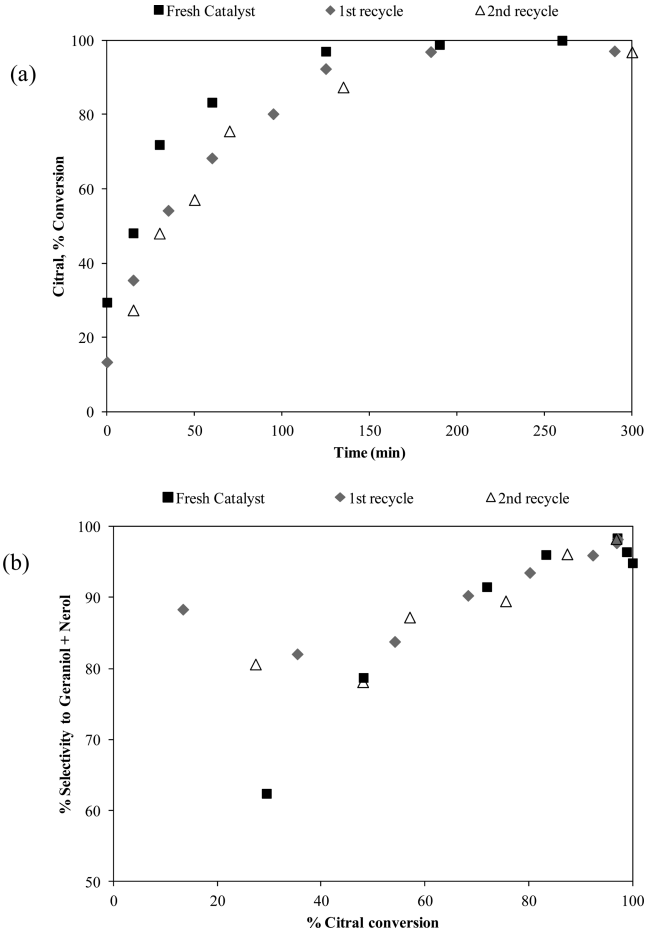

Figure 3. (a) Percent conversion to products for the hydrogenation of citral: ■, fresh catalyst; ♦, after first recycle; and Δ, after a second recycle as a function of reaction time; and (b) percent selectivity to geraniol/nerol for ■, fresh catalyst; ♦, after first recycle; and Δ, after a second recycle as a function of conversion to products. Reaction conditions: citral, 0.02 mol; solvent, 60 cm^3 (10 mol % 2-propanol in water); 5% Pt/SiO_2 catalyst, 0.3 g (particle size <45 μm); 100 °C; H_2 pressure, 1 MPa; stirrer speed, 1500 rpm.

thought that the spectra obtained using the catalyst film are dominated by liquid phase citral in the catalyst pores or the interparticle void volume of the catalyst powder film. In contrast, when the catalyst was exposed to the citral/2-propanol feed for only a short time (Figure 5), changes in the relative intensities of the bands were detected when compared with the pure liquid phase spectra. For example, the spectra observed 81 s following the switch in feed showed that the ν(C═O) bands at 1667/1681 cm^{-1} (trans/cis C═O citral, respectively; the cis and trans ν(C═C) bands occur at 1610/1634 cm^{-1}) were of comparable intensity to the bands found at 1379 and 1396 cm^{-1} due to $\delta(CH_3)_{sym}$ and aldehyde C−H rock, respectively.[25,26] A band at 1027 cm^{-1} was also observed 81 s after switching the feed, which over 4 min of exposure became more intense than the C−H deformation bands (SI Figure S1). In the citral spectrum in the absence of the catalyst, that is, the uncoated ZnSe IRE crystal, the bands in this region are of much lower intensity than the alkane deformation bands, which shows that significant intensity enhancement occurs in these spectra. Furthermore, other bands of citral (for example, the band at 1195 cm^{-1}) were not detected at this exposure time. The enhanced intensity of these bands relative to the C═O band over the catalyst film (Figures 5 and SI S1), which is normally the most intense band in the citral spectrum, suggests that these bands are associated with adsorbed citral or that the reduction in intensity of the C═O band is associated with binding of the aldehydic part of the molecule. The changes in the STOS spectra with exposure time are striking and show that it is possible to differentiate between citral adsorbed on a real catalyst and the dissolved citral in the liquid phase within the catalyst pores/interparticle void volume.

Of course, although the short time-on-stream ATR-IR spectroscopy has clearly identified bands due to adsorbed citral, as opposed to liquid phase citral, these adsorbed species may not be on the metal sites. In fact, the DRIFT spectra indicated that significant adsorption on the support was possible from the gas phase. To elucidate where the citral was adsorbing and, thus, to be able to comment on the mode of the adsorption, CO(g)-saturated 2-propanol was passed over the catalyst to block the Pt sites.[24] A Pt−CO band at 2075 cm^{-1} due to linearly adsorbed

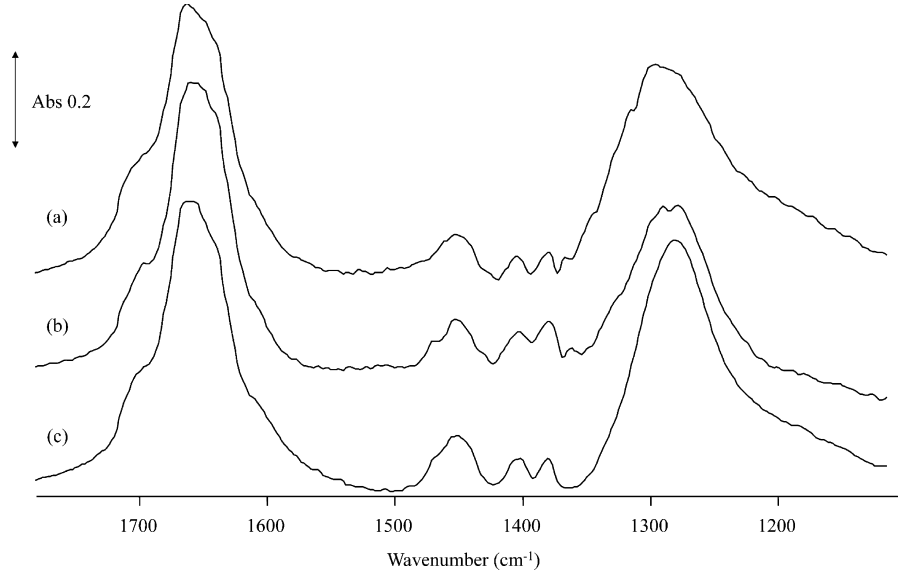

Figure 4. DRIFT spectra of citral adsorbed on (a) SiO_2, (b) Pt/SiO_2, and (c) Pt/SiO_2 after adsorption of CO.

dx.doi.org/10.1021/cs500185n | ACS Catal. 2014, 4, 2470−2478

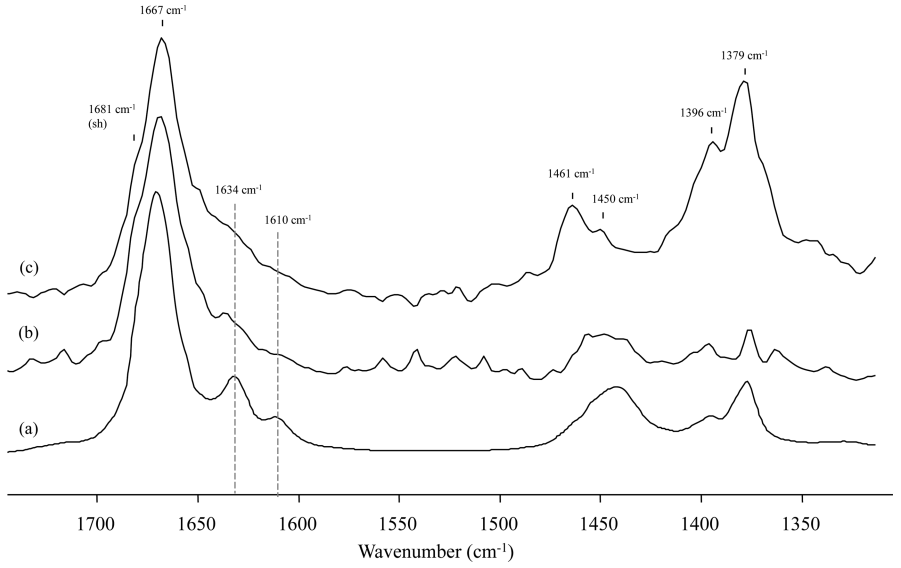

Figure 5. ATR-IR spectra normalized to the ν(C═O) band at 1667 cm^{-1} of (a) citral over a blank ZnSe, (b) 0.1 M citral in 2-propanol over a ZnSe IRE 81 s exposure to the feed (short time-on-stream ATR-IR spectrum) and (c) over Pt/SiO_2, 81 s exposure to the feed (short time-on-stream ATR-IR spectrum). Bands due to 2-propanol have been subtracted from all spectra.

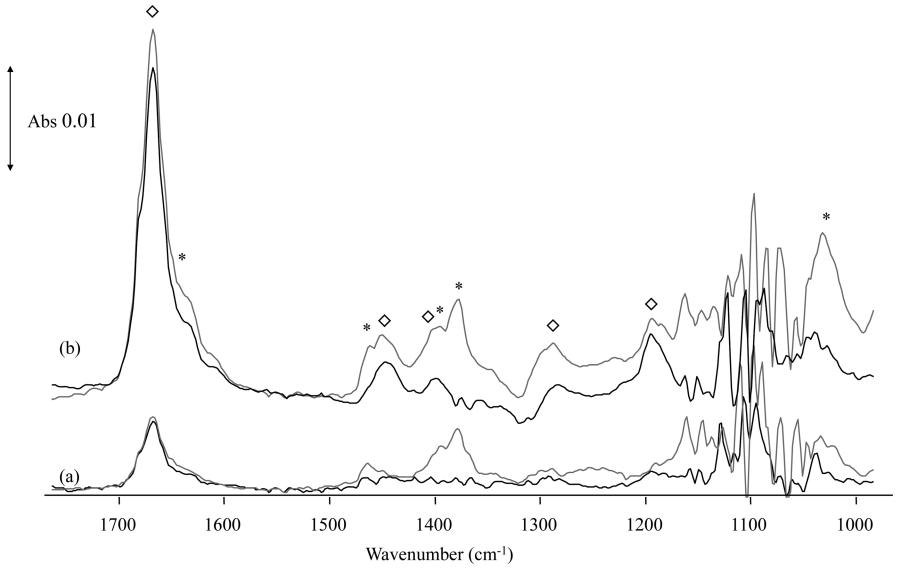

Figure 6. Short time-on-stream ATR-IR spectra of 0.1 M citral in 2-propanol over Pt/SiO_2 (gray spectra) and CO-Pt/SiO_2 (black spectra) after (a) 81 s for Pt/SiO_2 and 108 s of exposure for CO-Pt/SiO_2 and (b) 4 min of exposure for both Pt/SiO_2 and CO-Pt/SiO_2. Bands due to 2-propanol have been subtracted. ◇, bands due to citral adsorbed on support; *, bands due to citral adsorbed on Pt.

CO was observed, and this band was retained following a purge with 2-propanol, showing strong adsorption of CO on the Pt. The feed was then switched to 0.1 M citral/2-propanol, and SI Figure S2 shows the change with time over CO-Pt/SiO_2 following the switch. Clear differences are observable, even after 4 min of exposure to the citral-containing feed, as compared with those obtained for citral adsorbed on Pt/SiO_2 without pre-exposure to CO (Figure 5 and SI S1).

A comparison of spectra following citral adsorption 81 s and 4 min after the switch in the feed on Pt/SiO_2 and CO−Pt/SiO_2 is shown in Figure 6. After 81 s, only bands at 1668 and1632/1607 cm^{-1} were observed in the CO−Pt/SiO_2 spectra, whereas in the Pt/SiO_2 spectra, bands at 1461, 1450, 1396, 1379, and 1027 cm^{-1} were also observed (Figure 6a). It is evident that bands that are present on Pt/SiO_2 are lost when CO is preadsorbed on the catalyst, indicating that these bands are related to adsorbed citral species on Pt and not on the support. After 4 min of exposure to the feed, the 1668 cm^{-1} band in the spectra over the CO−Pt/SiO_2 catalyst was found to increase in intensity, with additional bands at 1450, 1401, and 1195 cm^{-1} also being observed to grow (Figure 6b). These bands are also present after 4 min of exposure over Pt/SiO_2 and are proposed to be due to adsorption of citral on the silica support. These spectral features are not likely to be due to liquid phase citral because if this were the case, all the bands would be expected to occur with the same relative intensities as in the reference liquid phase spectrum, and this is not found. For example, the peak at 1379 cm^{-1} is relatively much weaker in the spectrum after 4 min of exposure compared with that after 15 min of exposure to the feed, that is, when the spectrum has more of a contribution

dx.doi.org/10.1021/cs500185n | ACS Catal. 2014, 4, 2470−2478

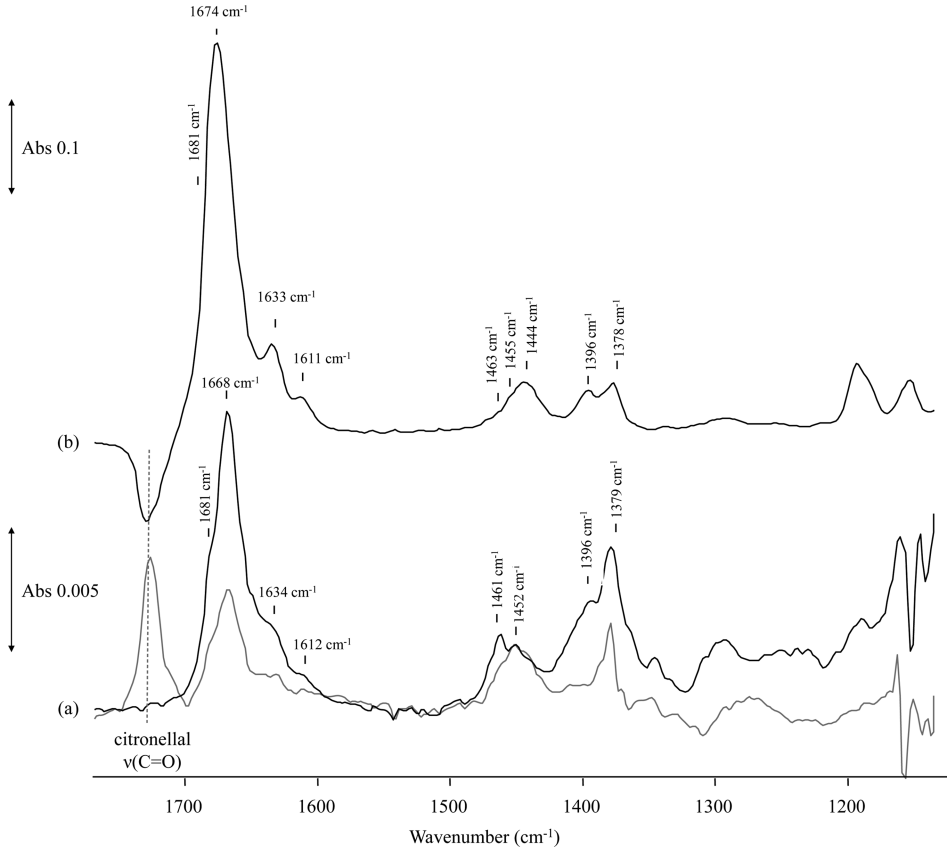

Figure 7. ATR-IR spectra of 0.1 M citral in 2-propanol on Pt/SiO_2 after 25 min of exposure to 0.1 M citronellal in 2-propanol. (a) Black spectrum: citral adsorption 81 s after switching feed (no preadsorption of citronellal). Gray spectrum: citral adsorption 81 s after switching feed for Pt/SiO_2 with adsorbed citronellal. (b) Citral adsorbed 25 min after switching the feed for Pt/SiO_2 with adsorbed citronellal. Bands due to adsorbed citronellal/2-propanol have been subtracted.

from the liquid in the pore (SI Figure S2b). In addition, changes in the region 1000−1200 cm^{-1} are observed. However, these are relatively small changes, indicating a weak interaction with the support, as compared with the Pt; thus, it is difficult to determine the mode of adsorption.

A contribution to the C═O region of the spectra with and without adsorbed CO is also observed. Citral adsorbed on Pt/SiO_2 has a contribution at 1649 cm^{-1}, a shoulder between the 1667 cm^{-1} ν(C═O) band and the 1634/1610 cm^{-1} ν(C═C) bands of citral that suggests a weakly perturbed C═O band in the adsorbed citral molecule. When CO was preadsorbed, the 1649 cm^{-1} contribution was lost, together with the bands at 1461, 1396, 1379, and 1027 cm^{-1}. All of these bands are related to citral adsorption on Pt.

It should be noted that in the period immediately following a switch from 2-propanol to 0.1 M citral in 2-propanol, the initial citral concentration in the flow cell will be significantly less than 0.1 M. As the citral solution flows, the concentration of citral molecules in the catalyst layer will increase until the layer (Pt + support) is saturated. Spectra recorded after switching to the citral feed are, therefore, effectively taken over an increasing concentration range. In the first few spectra after the switch, that is, as the concentration in the feed on the surface of the catalyst increases, there is no significant change in the citral bands observed. The bands change only where it is thought that the support adsorption/pore filling dominates, which indicates that there is no significant effect on the spectra as a function of the surface citral concentration on the metal.

The hydrogenation results showed that adsorbed citronellal alters the interaction of citral with the catalyst, thus enhancing C═O hydrogenation. STOS-ATR-IR spectra probing the perturbation in citral adsorption following preadsorption of citronellal were studied. The catalyst was pre-exposed to 0.1 M citronellal/2-propanol for 25 min (SI Figure S3) before switching the feed to 0.1 M citral in 2-propanol. When citral is adsorbed on the as-received catalyst, bands at 1634, 1461, 1396, 1379, and 1027 cm^{-1} are observed in the spectra as a result of citral adsorbed on Pt (Figures 5 and 7a). However, when citral is adsorbed on the catalyst pre-exposed to citronellal, there is loss of the band at 1394 cm^{-1} (aldehyde C−H rock) and some loss of intensity at 1462 and 1379 cm^{-1} (CH_3 asym/sym deformation) (Figure 7a). The absence of the band associated with the aldehydic C−H suggests that the C═O group is adsorbing. This is consistent with the higher selectivity to geraniol/nerol observed in the reaction spiked with citronellal. In the spectrum observed 81 s after the switch, the band associated with support adsorption at ∼1450 cm^{-1} is of comparable intensity in the two spectra, yet the C═O band is of significantly weaker intensity for citral after citronellal adsorption (Figure 7a). The spectra due to citral adsorption at long exposure times after switching the feed show this band at 1396 cm^{-1}, which is due to either citral in the liquid phase or citral adsorption because citronellal desorbs under flow (Figure 7b).

Spiking the reaction with citronellal gave 97% selectivity to geraniol/nerol from the start of the reaction, and in the STOS-ATR-IR spectra, citral, following preadsorption of citronellal, is

dx.doi.org/10.1021/cs500185n | ACS Catal. 2014, 4, 2470−2478

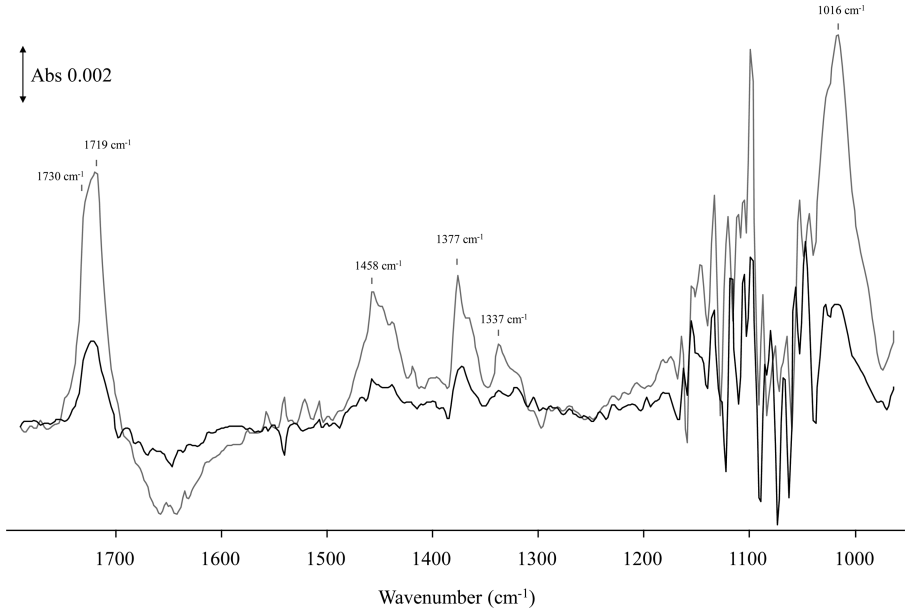

Figure 8. Short time-on-stream ATR-IR spectra of 0.1 M citronellal in 2-propanol on Pt/SiO_2: after 108 s (black spectrum) and 4 min (gray spectrum) of exposure to the citronellal solution. Bands due to 2-propanol have been subtracted.

found to preferentially adsorb through the C═O group. For the reaction without spiking, the initial selectivity in the reaction is 70% to C═O and 30% to C═C hydrogenation. STOS-ATR-IR spectra of citral without citronellal present show the band at 1394 cm^{-1}, which suggests that citral adsorbs through both the C═O and C═C groups either separately as η_2 modes (di-$\sigma_{(CC)}$ or η_2 di-$\sigma_{(CO)}$) or through both groups in an η_3 (di-$\sigma_{(CC)}$−$\sigma_{(O)}$) or η_4 (di-$\sigma_{(CC)}$ + di-$\sigma_{(CO)}$) mode.[24,25] We postulate that at the start of the reaction, citral adsorption on Pt can occur through both η_3 (di-$\sigma_{(CC)}$−$\sigma_{(O)}$) and η_2 (di-$\sigma_{(CO)}$) adsorption modes. If interaction of the C═C bond of citral with Pt was through an η_4 (di-$\sigma_{(CC)}$ + di-$\sigma_{(CO)}$) mode, bands due to aldehydic species would not be expected in the spectra of citral on Pt, which is not the case. The weakly perturbed C═O band at 1649 cm^{-1} observed for citral adsorbed on Pt is associated with the η_3 (di-$\sigma_{(CC)}$−$\sigma_{(O)}$) mode; the band at 1027 cm^{-1}, with the C−O (single bond character) of an η_2 di-$\sigma_{(CO)}$ mode hydrogen-bonded with the 2-propanol. The C−O stretch of an alcohol would be found in this region.[27]

Citral adsorption at the start of the reaction, through individual C═C and C═O adsorption modes results in the formation of citronellal and geraniol/nerol. As the reaction proceeds, the citronellal formed initially adsorbs on Pt. STOS-ATR-IR spectra of 0.1 M citronellal/2-propanol adsorption show a band at 1016 cm^{-1} that is of greater intensity than the ν(C═O) bands at 1731/1718 cm^{-1} (Figure 8). This 1016 cm^{-1} band is proposed to be due to citronellal adsorbed in an η_2 (di-$\sigma_{(CO)}$) mode hydrogen bonded with 2-propanol, analogous to the η_2 (di-$\sigma_{(CO)}$) citral band at 1027 cm^{-1}. The most stable adsorption mode of C_1−C_4 aldehydes has been calculated from DFT to be the η_2 (di-$\sigma_{(CO)}$) mode.[28]

The adsorption of citronellal alters the subsequent adsorption of citral in the reaction, which causes the change in selectivity as the reaction proceeds, providing enhanced C═O hydrogenation. When citronellal is present in the system from the start of the reaction (recycling the catalyst as well as the spiking experiments), citral adsorption on the Pt through the C═C bond (η_3 (di-$\sigma_{(CC)}$−$\sigma_{(O)}$) mode) does not occur, and hence, higher selectivity for C═O hydrogenation is observed (Scheme 2).

Scheme 2. Schematic of Citral Adsorption Modes and the Influence of Citronellal on the Reaction Selectivity

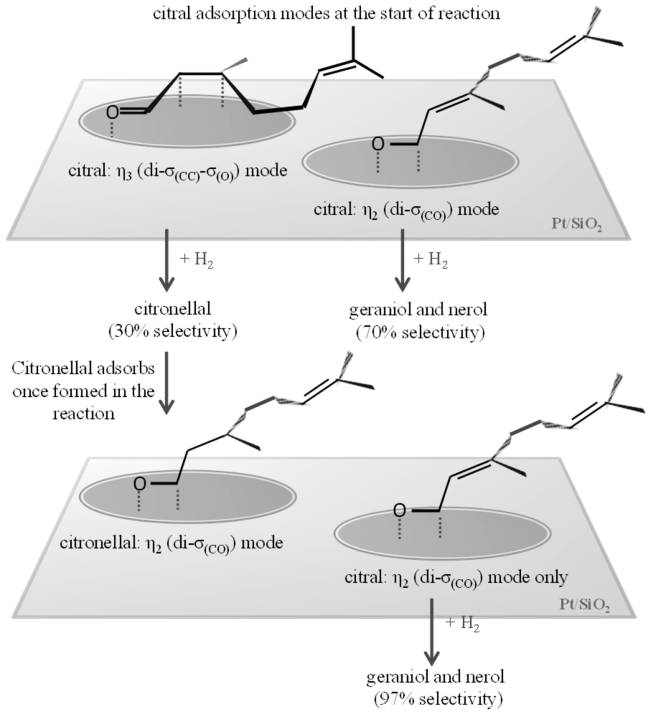

These results can be compared with the changes in citral hydrogenation on other Pt-based catalysts following adsorption of organic modifiers. Using Pt_3Co nanocrystals capped with aliphatic amines, with increasing chain length of the amine from butyl amine to octadecylamine, the rate decreased significantly, but importantly, the selectivity to the C═O hydrogenation versus the C═C reduction was enhanced.[7] This was attributed

dx.doi.org/10.1021/cs500185n | ACS Catal. 2014, 4, 2470−2478

to the long alkyl chain amines stopping the C=C bond from interacting with the surface as a consequence of steric hindrance, forcing the citral to adsorb in a tilted geometry through the C=O bond only. Kahsar et al. demonstrated that thiols interacting with Pt/Al_2O_3 could also lead to enhanced selectivity for the unsaturated alcohol in the case of cinnamaldehyde and prenal.[8] In both cases, this effect was attributed to noncovalent interactions changing the adsorption geometry compared with the uncoated catalyst. Interestingly, although little effect was found on comparing aromatic and aliphatic thiols in the case of prenal hydrogenation, further increases in selectivity were observed for the case of cinnamaldehyde, which is reported to be due to $\pi-\pi$ interactions between the substrate and the coating. Although similar effects are found between the results reported herein and these studies, it is important to note the large differences in the adsorption strengths in each case, from the very strong thiol binding to the weakly bound citronellal in the present study. This illustrates that such effects are a general phenomenon and are likely to occur in many selective reactions of multifunctional molecules.

CONCLUSIONS

STOS-ATR-IR spectroscopy has allowed us to investigate the adsorption mode of citral on Pt, even when adsorption on the silica support is possible and eventually dominates the spectra. Using this technique, we have identified a possible explanation for why the selectivity in the citral hydrogenation reaction changes as the reaction proceeds. It appears that the formation of a product (such as citronellal) can modify the adsorption of the citral and force the reaction down one particular pathway, leading to very high selectivity to geraniol and nerol.

ASSOCIATED CONTENT

Supporting Information

Overlaid ATR-IR spectra following switching in a 0.1 M citral solution over a untreated and CO treated Pt/SiO_2 catalyst. Overlaid ATR-IR spectra following switching in a 0.1 M citronellal solution over a untreated. Pt/SiO_2 catalyst characterization: BET, XRD, and TEM. This material is available free of charge via the Internet at http://pubs.acs.org.

AUTHOR INFORMATION

Corresponding Author

*E-mail: c.hardacre@qub.ac.uk.

Notes

The authors declare no competing financial interest.

ACKNOWLEDGMENTS

We acknowledge EPSRC for funding as part of the CASTech Grant (EP/G011397/1).

REFERENCES

(1) (a) Stolle, A.; Gallert, T.; Schmöger, C.; Ondruschka, B. *RSC Adv.* **2013**, *3*, 2112−2153. (b) Singh, U. K.; Vannice, M. A. *J. Catal.* **2000**, *190*, 165−180. (c) Singh, U. K.; Sysak, M. N.; Vannice, M. A. *J. Catal.* **2000**, *191*, 181−191. (d) Mukherjee, S.; Vannice, M. A. *J. Catal.* **2006**, *243*, 108−130. (e) Mukherjee, S.; Vannice, M. A. *J. Catal.* **2006**, *243*, 131−148.

(2) (a) Ponec, V. *Appl. Catal., A* **1997**, *149*, 27−48. (b) Hirschl, R.; Delbecq, F.; Sautet, P.; Hafner, J. *J. Catal.* **2003**, *217*, 354−366. (c) Delbecq, F.; Sautet, P. *J. Catal.* **2003**, *220*, 115−126. (d) Vilella, I. M. J.; de Miguel, S. R.; Scelza, O. A. *J. Mol. Catal. A* **2008**, *284*, 161−171. (e) Siani, A.; Alexeev, O. S.; Lafaye, G.; Amiridis, M. D. *J. Catal.* **2009**, *266*, 26−38. (f) Stassi, J. P.; Zgolica, P. D.; de Miguel, S. R.; Scelza, O. A. *J. Catal.* **2013**, *306*, 11−29.

(3) Marshall, S. T.; O'Brien, M.; Oetter, B.; Corpuz, A.; Richards, R. M.; Schwartz, D. K.; Medlin, J. W. *Nat. Mater.* **2010**, *9*, 853−858.

(4) Makosch, M.; Lin, W.-I.; Bumbalek, V.; Sa, J.; Medlin, J. W.; Hungerbuhler, K.; van Bokhoven, J. A. *ACS Catal.* **2012**, *2*, 2079−2081.

(5) Álvarez-Rodríguez, J.; Guerrero-Ruiz, A.; Arcoya, A.; Rodríguez-Ramos, I. *Catal. Lett.* **2009**, *129*, 376−382.

(6) Jiang, H.-J.; Jiang, H.-B.; Zhu, D.-M.; Zheng, X.-L.; Fu, H.-Y.; Chen, H.; Li, R.-X. *Appl. Catal., A* **2012**, *445−446*, 351−358.

(7) Wu, B.; Huang, H.; Yang, J.; Zheng, N.; Fu, G. *Angew. Chem., Int. Ed.* **2012**, *51*, 3440−3443.

(8) Kahsar, K. R.; Schwartz, D. K.; Medlin, J. W. *J. Am. Chem. Soc.* **2014**, *136*, 520−526.

(9) (a) Burgi, T.; Baiker, A. *Adv. Catal.* **2006**, *50*, 227−283. (b) Burgi, T. *J. Catal.* **2005**, *229*, 55−63. (c) Ebbesen, S. D.; Mojet, B. L.; Lefferts, L. *J. Catal.* **2008**, *256*, 15−23. (d) Keresszegi, C.; Ferri, D.; Mallat, T.; Baiker, A. *J. Phys. Chem. B* **2005**, *109*, 958−967. (e) Burgener, M.; Wirz, R.; Mallat, T.; Baiker, A. *J. Catal.* **2004**, *228*, 152−161. (f) Andason, J.-M.; Baiker, A. *Chem. Soc. Rev.* **2010**, *39*, 4571−4584.

(10) (a) Meier, D. M.; Mallat, T.; Ferri, D.; Baiker, A. *J. Catal.* **2006**, *244*, 260−263. (b) Ferri, D.; Bürgi, T.; Baiker, A. *J. Phys. Chem. B* **2001**, *105*, 3187−3195.

(11) Ebbesen, S. D.; Mojet, B. L.; Lefferts, L. *Langmuir* **2008**, *24*, 869−879.

(12) Ortiz-Hernandez, I.; Williams, C. T. *Langmuir* **2003**, *19*, 2956−2962.

(13) Meier, D. M.; Ferri, D.; Mallat, T.; Baiker, A. *J. Catal.* **2007**, *248*, 68−76.

(14) Burgi, T.; Bieri, M. *J. Phys. Chem. B* **2004**, *108*, 13364−13369.

(15) (a) Maeda, N.; Hungerbühler, K.; Baiker, A. *J. Am. Chem. Soc.* **2011**, *133*, 19567−19659. (b) Meemken, F.; Maeda, N.; Hungerbühler, K.; Baiker, A. *Angew. Chem., Int. Ed.* **2012**, *51*, 8212−8216.

(16) Richner, G.; van Bokhoven, J. A.; Neuhold, Y.-M.; Makosch, M.; Hungerbühler, K. *Phys. Chem. Chem. Phys.* **2011**, *13*, 12463−12471.

(17) Sun, X.; Williams, C. T. *Catal. Commun.* **2012**, *17*, 13−17.

(18) Burgi, T. *J. Catal.* **2005**, *229*, 55−63.

(19) Copeland, J. R.; Foo, G. S.; Harrison, L. A.; Sievers, C. *Catal. Today* **2013**, *205*, 49−59.

(20) Chansai, S.; Burch, R.; Hardacre, C.; Breen, J.; Meunier, F. C. *J. Catal.* **2011**, *281*, 98−105. (b) Chansai, S.; Burch, R.; Hardacre, C. *J. Catal.* **2012**, *295*, 223−231.

(21) Chatterjee, A.; Chatterjee, M.; Ikushima, Y.; Mizukami, F. *Chem. Phys. Lett.* **2004**, *395*, 143−149.

(22) Pak, A. M.; Vozdvizhenskii, V. F.; Turganbaeva, S. M.; Levintova, T. D.; Konuspaev, S. R. *React. Kinet. Catal. Lett.* **1983**, *23*, 1−5.

(23) Burgener, M.; Wirz, R.; Mallat, T.; Baiker, A. *J. Catal.* **2004**, *228*, 152−161.

(24) Ferri, D.; Mondelli, C.; Krumeich, F.; Baiker, A. *J. Phys. Chem. B* **2006**, *110*, 22982−22986.

(25) (a) Colthup, N. B.; Daly, L. H.; Wiberley, S. E. *Introduction to Infrared and Raman Spectroscopy*; Academic Press: New York, 1975. (b) Haubrich, J.; Loffreda, D.; Delbecq, F.; Sautet, P.; Jugnet, Y.; Krupski, A.; Becker, C.; Wandelt, K. *J. Phys. Chem. C* **2008**, *112*, 3701−3718. (c) Dandekar, A.; Vannice, M. A. *J. Catal.* **1999**, *183*, 344−354. (d) Silvestre-Albero, J.; Sepúlveda-Escribano, A.; Rodríguez-Reinoso, F.; Anderson, J. A. *Phys. Chem. Chem. Phys.* **2003**, *5*, 208−216.

(26) (a) Delbecq, F.; Sautet, P. *J. Catal.* **2002**, *211*, 398−406. (b) Kliewer, C. J.; Bieri, M.; Somorjai, G. A. *J. Am. Chem. Soc.* **2009**, *131*, 9958−9966.

(27) Merlo, A. B.; Santori, G. F.; Sambeth, J.; Siri, G. J.; Casella, M. L.; Ferretti, O. A. *Catal. Commun.* **2006**, *7*, 204−208.

(28) Sinha, N. K.; Neurock, M. *J. Catal.* **2012**, *295*, 31−44.